

Sputtering and Luminescence in Electronically Excited Solid Argon

C. T. Reimann and R. E. Johnson

Department of Nuclear Engineering and Engineering Physics, University of Virginia, Charlottesville, Virginia 22901

and

W. L. Brown

AT&T Bell Laboratories, Murray Hill, New Jersey 07974

(Received 29 February 1984)

We have measured both ultraviolet luminescence and ejection of atomic argon from solid argon films electronically excited by megaelectronvolt light ions. The two phenomena reflect (respectively) the radiative and the nonradiative parts of the energy release during electronic recombination and deexcitation. The measurements can be correlated by a model of diffusion of ionic excitons followed by formation and decay of self-trapped excimers.

PACS numbers: 79.20.Nc, 71.35.+z

In this paper we show that atomic ejection and luminescence from electronically excited solid argon are different manifestations of the decay of excitons to the ground state. This is made evident by a correlation between the thickness dependences of the sputtering and luminescence yields of solid argon bombarded by megaelectronvolt light ions.

Electronic excitation of rare-gas solids is known to produce ultraviolet luminescence through rapid self-trapping of excitons to form localized excimers.¹ These excimers decay radiatively in $\sim 10^{-9}$ – 10^{-6} sec.^{2,3} A substantial part of the total energy of free excitons is, however, not released as radiation. It is transferred nonradiatively to the lattice through multiphonon relaxation³ and repulsive electronic deexcitation processes.⁴ The proposed decay sequence⁴ is shown schematically in Fig. 1. In the return of a single ionization event to the ground state in pure solid argon there are expected to be fast nonradiative ~ 1 – 2 -eV repulsive energy releases both before⁴ and after^{3,5} the radiative decay. If such repulsive energy releases occur sufficiently close to the surface they can result in ejection of atoms from the surface, since the sublimation energy of surface argon atoms is only ~ 0.08 eV.

High sputtering yields (atoms lost from the film per incident ion) have been reported for rare-gas solids bombarded by megaelectronvolt ions,^{6,7} and exciton diffusion and decay have been suggested as a means of accounting for the dependence of sputtering yield on film thickness reported for both argon and xenon films.⁵ The rare-gas solids are special cases of a broad range of insulating solids which exhibit sputtering under electronic excitation.^{8–11} These phenomena are entirely separate from the common sputtering of metals and narrow-band-gap semiconductors which arises from

momentum-transferring collisions of an incident ion with atoms of a solid.¹²

Argon ice layers with thicknesses between 100 and 2000 Å were grown by admitting argon gas into an ultrahigh-vacuum target chamber with a gold-on-beryllium target cooled to ~ 12 K. Absolute film thicknesses and sputtering yields were measured by Rutherford backscattering (RBS) which

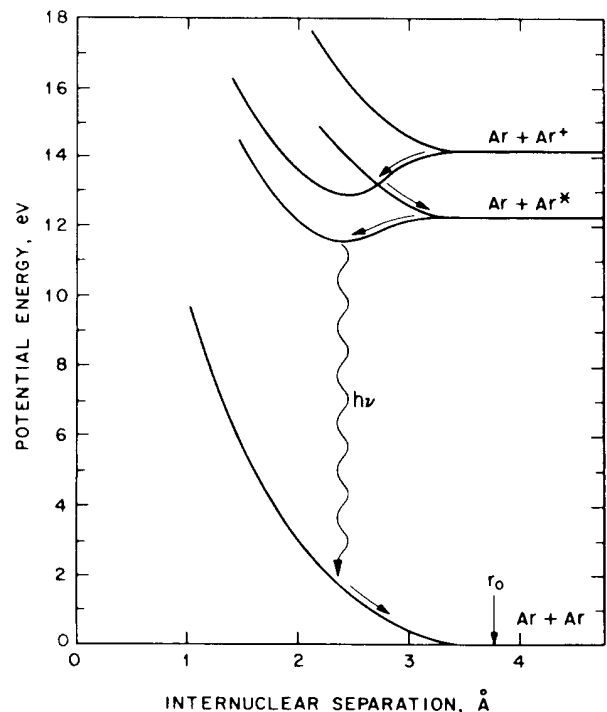


FIG. 1. Typical interatomic potentials in solid Ar. Binding energies, equilibrium internuclear separations from gas phase; free exciton energies from solid phase; Schwentner, Koch, and Jortner, Ref. 3. Shapes are approximate.

directly determines the atomic thickness of the films.⁸ However, all of the luminescence results and many of the sputtering results to be reported are relative yields obtained by use of a quadrupole mass spectrometer (QMS). The thin-film argon target is on the axis of the QMS and part of the entrance cone of the channeltron detector of the QMS is directly exposed to ultraviolet radiation from the target. Since this uv gives an equal signal at all mass settings of the QMS a dummy mass setting (e.g., 7 amu) is used to monitor the luminescence yield. The signal for mass 40 amu, corresponding to sputtered argon atoms, is corrected for this uv contribution to obtain the sputtered-particle yield alone. The yields are independent of beam-current density in the range of the experiment.

Figure 2(a) shows RBS measurements of the thickness dependence of sputtering yield for 1.5-

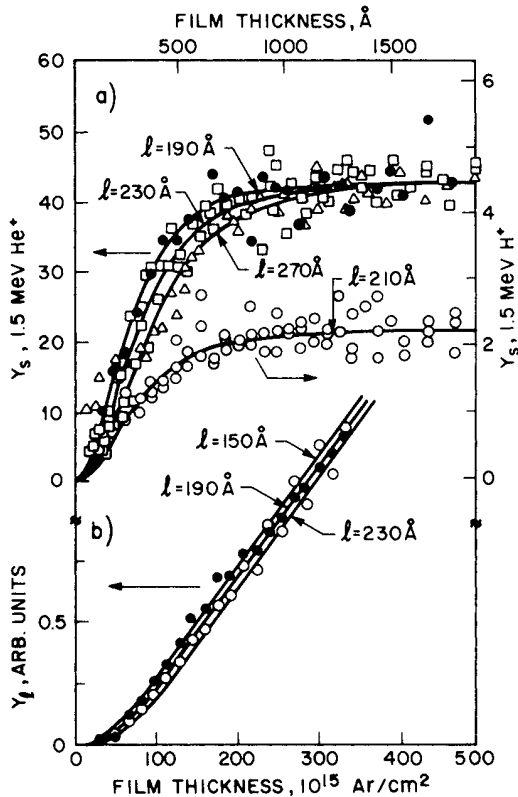


FIG. 2. (a) Thickness dependence of sputtering yields. Open squares, 1.5-MeV He⁺, RBS; filled circles, 1.5-MeV He⁺, QMS; open circles, 1.5-MeV H⁺, QMS; open triangles, Besenbacher *et al.*, Ref. 6, 750-keV He⁺ RBS. All He⁺ yields normalized to 1.5-MeV He⁺ RBS. The H⁺ yield scale is determined from absolute He⁺ RBS yields by comparison of QMS H⁺ and He⁺ yields. (b) Thickness dependence of luminescence yields. Open circles, 1.5-MeV H⁺; filled circles, 1.5-MeV He⁺. Solid lines in (a) and (b) are fits by model in the text.

MeV He⁺ in comparison with data from Besenbacher *et al.*⁶ for 750-keV He⁺. Also shown in Fig. 2(a) are our QMS measurements for 1.5-MeV H⁺ and He⁺. The shapes of the QMS and RBS curves are quite similar. Furthermore, the shape of the thickness dependence for incident H⁺ is the same as that for He⁺ within the scatter in the data even though the energy densities deposited by these ions along their paths through the argon differ by about a factor of 10. Figure 2(b) shows data for the luminescence yield.

To account for the luminescence and sputtering behavior we utilize the main features of Fig. 1. We assume that the incident ions predominantly produce ionic excitons (hole-electron pairs, ion-electron pairs).¹³ These carry out ambipolar diffusion until the Ar⁺ ion relaxes with a neighboring atom to form the self-trapped species Ar₂⁺. Through level crossings, the Ar₂⁺ and an electron recombine to form an Ar* exciton with kinetic energy.⁴ The total energy release in the relaxation and subsequent repulsion is ~1–2 eV.³ The atomic exciton then relaxes with a neighbor to form a vibrationally excited Ar₂^{*} excimer. Because the Ar* is created with kinetic energy we assume that it is trapped close to its production site. The fast trapping (~10⁻¹⁴ sec) can occur essentially through an energetic three-body collision of the Ar* with two atoms of the solid rather than via the much slower multiphonon process involved in trapping a near-thermal exciton. As a result of the lack of level crossing, the Ar₂^{*} excimer vibrationally relaxes to its ground state via multiphonon emission and then radiates a characteristic ~9.8-eV photon.¹ Following the luminescence there is a further release of ~1.6-eV repulsive energy because of the close spacing of the argon atoms that existed in the Ar₂^{*} excimer.^{3,5}

If we ignore exciton-exciton interactions, one-dimensional time-independent diffusion equations describe the spatial distribution of ionic excitons and excimers during steady-state excitation by an ion beam of current density I₀, giving a depth-independent volume generation rate α₊I₀ of hole-electron pairs:

$$D_+ \frac{d^2 n_+}{dx^2} - \frac{n_+}{\tau_+} + \alpha_+ I_0 = 0; \quad \frac{n_+}{\tau_+} - \frac{n_*}{\tau_r} = 0.$$

In these expressions, ionic excitons have a density n₊ and a diffusion coefficient D₊. The density of excimers is n*. τ₊ is the self-trapping time for the ionic excitons which have a diffusion length l = (D₊τ₊)^{1/2}. τ_r is the radiative lifetime of the excimer. The boundary conditions on the diffusing

excitons at the surface ($x=0$) and the metal ($x=d$) interface are represented by

$$D_+ [dn_+/dx]_0 = \Delta_0(l/\tau_+)n_+(0), \quad D_+ [dn_+/dx]_d = -\Delta_d(l/\tau_+)n_+(d),$$

where Δ_0 and Δ_d are recombination velocities in units of l/τ_+ . The sputtering and luminescence yields then become

$$Y_s = \frac{1}{I_0} \int_0^d \frac{n_+(x)}{\tau_+} \Lambda_+(x) dx + \frac{1}{I_0} \int_0^d \frac{n_*(x)}{\tau_r} \Lambda_*(x) dx + \frac{1}{I_0} D_+ \frac{dn_+}{dx} \Big|_0 [\Lambda_+(0) + \Lambda_*(0)],$$

$$Y_l = \frac{1}{I_0} \int_0^d \frac{n_*(x)}{\tau_r} dx + \frac{1}{I_0} D_+ \frac{dn_+}{dx} \Big|_0.$$

In Y_s the first term is from repulsive recombination of Ar_2^+ to form Ar^* , and the second term is from repulsive separation of two ground-state Ar atoms after the radiative decay of Ar_2^+ . These processes occurring in the near-surface bulk of the film cause sputtering according to the weighting functions $\Lambda_+(x)$ and $\Lambda_*(x)$. The third term is from exciton trapping at the surface. In Y_l , the two terms are from radiative decay in the bulk and at the surface. Since the luminescent photon, with an energy of 9.8 eV, is Stokes shifted by ~ 2 eV from the lowest absorption energy of solid argon,¹ photons escape from any depth.

The thickness dependences of Y_s and Y_l are highly insensitive to the shapes of $\Lambda_+(x)$ and $\Lambda_*(x)$ as long as the latter fall off within a distance short compared to the diffusion length l . From computer simulation,¹⁴ ejection depths are estimated to be ~ 10 Å, small compared to diffusion lengths experimentally determined below. We represent $\Lambda_+(x)$ and $\Lambda_*(x)$ as decreasing exponentials with 10-Å characteristic decays. For energy inputs of 2 and 1.6 eV for the upper and lower decays, respectively, the computer simulation gave $\Lambda_+(0) = 2.0$ and $\Lambda_*(0) = 1.2$ ejected atoms per decay.

This exciton diffusion and decay model is fitted to our sputtering data. We have found that the boundary conditions $\Delta_0 = 0$ and $\Delta_d = \infty$ are appropriate as will be discussed below. We obtain values of l from the fits in the range of 190 to 230 Å. Besenbacher's data give a somewhat higher value, 270 Å. Fits to our luminescence data give l in the range 150 to 230 Å. Overall, the model correlates the luminescence and sputtering thickness dependence with $l = 190 \pm 40$ Å. This length is much larger than $l = 50$ Å of $n = 1$ excitons in Ar.³ In Kr, the diffusion length has been reported to increase from 30 Å for $n = 1$ to 300 Å for $n = 2$ excitons.¹⁵ The relatively large values we obtain for diffusion length in Ar support our premise that the diffusing species is an ionic exciton or very highly excited atomic exciton and not the vibrationally ex-

cited excimer, as has been suggested.⁵

$\Delta_0 = 0$ means that the vacuum interface reflects excitons, a boundary condition which has been determined for excitons in krypton ice.¹⁵ The model predicts that the shape of the Y_s thickness dependence is not very sensitive to Δ_0 , although the predicted magnitude of Y_s is. To determine Δ_0 , we assume that the ionic exciton source function is S_e/W , where S_e is the electronic stopping power and W is the average energy expended to make a hole-electron pair. Comparison of the measured thick-film sputtering yield with the value predicted by the model then gives $\Delta_0 \leq 0.03$. The fits in Fig. 2 are not affected by such small nonzero values. Values in this range contradict the use of a trapping vacuum-interface boundary condition as in Ref. 5. $\Delta_d = \infty$ reflects the fact that the metal substrate acts as a nonradiative sink for excitons.¹⁶ The largeness of Δ_d is indicated by our data by noting that the ratio of the thickness for which $Y_s = 90\%$ of saturation to the thickness intercept of the linear part of Y_l is about 3. For all values of $\Delta_0 \leq 0.1$ the model predicts this ratio to be about 3 if $\Delta_d \geq 10$, which implies that the metal substrate is a good sink as assumed.

There are small deviations from linearity of luminescence and sputtering yield with the density of electronic excitation along individual particle paths and there are strong influences of impurities on both luminescence and sputtering yields. We are examining these phenomena in detail. However, for pure argon the experiments and model described above demonstrate that there is a simple connection between sputtering and luminescence in solid argon.

¹J. Jortner, L. Meyer, S. A. Rice, and E. G. Wilson, *J. Chem. Phys.* **42**, 4250 (1965).

²S. Kubota, M. Hishida, and J. Raun, *J. Phys. C* **11**,

2645 (1978).

³N. Schwentner, E. E. Koch, and J. Jortner, in "Rare Gas Solids, Vol. III," edited by M. L. Klein and J. A. Venables (Academic, New York, to be published).

⁴R. E. Johnson and M. Inokuti, Nucl. Instrum. Methods **206**, 289 (1983).

⁵C. Claussen, Ph.D. thesis, Odense Universitet, Odense, Denmark, 1982 (unpublished); P. Børgesen, J. Schön, H. Sørensen, and C. Claussen, Appl. Phys. A **29**, 57 (1982).

⁶F. Besenbacher, J. Bøttiger, O. Graversen, and J. L. Hansen, Nucl. Instrum. Methods **191**, 221 (1981).

⁷R. W. Ollerhead, J. Bøttiger, J. A. Davies, J. L'Ecuyer, H. K. Haugen, and N. Matsunami, Radiat. Eff. **49**, 203 (1980).

⁸W. L. Brown, W. M. Augustyniak, L. J. Lanzerotti, R. E. Johnson, and R. Evatt, Phys. Rev. Lett. **45**, 1632

(1980).

⁹J. E. Griffith, R. A. Weller, L. E. Seiberling, and T. A. Tombrello, Radiat. Eff. **51**, 223 (1980).

¹⁰R. E. Johnson and W. L. Brown, Nucl. Instrum. Methods **198**, 103 (1982).

¹¹J. P. Biersack and E. Santner, Nucl. Instrum. Methods **132**, 229 (1976); H. Overijnder, M. Szymanski, A. Haring, and A. DeVries, Radiat. Eff. **36**, 63 (1978); N. Itoh, Adv. Phys. **31**, 491 (1982).

¹²P. Sigmund, Phys. Rev. **184**, 383 (1969).

¹³J. Doke, A. Hitachi, S. Kubota, A. Nakamota, and J. Takahashi, Nucl. Instrum. Methods **134**, 353 (1976).

¹⁴B. Garrison and R. E. Johnson, to be published.

¹⁵N. Schwentner, G. Martens, and H. W. Rudolf, Phys. Status Solidi (b) **106**, 183 (1981).

¹⁶Z. Ophir, N. Schwentner, B. Raz. M. Skibowski, and J. Jortner, J. Chem. Phys. **63**, 1072 (1975).